



---

# Fully quantum description of a three level maser, driven by a thermal bath

---

Master-project

Sander Stammbach  
Prof. Patrick Potts  
Dr. Mateo Brunelli  
Marcelo Janovitch

12 November 2022

# Contents

<b>1</b>	<b>Introduction</b>	<b>2</b>
<b>2</b>	<b>System and model</b>	<b>3</b>
2.1	3-level-Maser Model . . . . .	3
2.2	Master-Equation . . . . .	4
<b>3</b>	<b>Methods</b>	<b>6</b>
3.1	Implementation of the three-level-system in qutip . . . . .	6
<b>4</b>	<b>Lasing transition</b>	<b>7</b>
4.1	Wigner function and phase-averaged coherent states . . . . .	7
4.2	Double threshold behaviour and population inversion . . . . .	10
<b>5</b>	<b>Thermodynamics</b>	<b>13</b>
5.1	Heat currents . . . . .	13
5.2	Entropy production . . . . .	15
<b>6</b>	<b>Conclusion and outlook</b>	<b>16</b>
<b>7</b>	<b>Appendix</b>	<b>18</b>
7.1	Software . . . . .	18

# 1 Introduction

One of the most important questions in thermodynamics is how to convert thermal energy into work. For such tasks there exist many classical engines, for example the steam machines or gasoline engines. Those ideas also generalize to quantum systems. In this master-project, a three-level maser, driven by the coupling of a hot and a cold bath is quantified. The three-level maser is a quantum heat engine (QHE). The work extraction from a classical heat engine is often a moving piston. But in this case it is a driving field. In the year 1916 Albert Einstein already discussed three ways of light-matter-interaction (spontaneous emission, absorption, and stimulated emission)[2]. In a paper from 1959. Scovil and Schulz-DuBois [5] investigated whether a laser is a heat engine. In this paper, they take a maser as a device to transform heat into coherent radiation, because heat can make a population inversion. In their thermodynamic analysis, they use a single-atom laser. They made a groundwork for emerging theory of quantum thermodynamics. In practice and also for the calculations, two different reservoirs are necessary. The high-temperature reservoir can be realized by a fast and accurate estimation of the thermal occupation of propagating microwave modes [4].

## 2 System and model

### 2.1 3-level-Maser Model

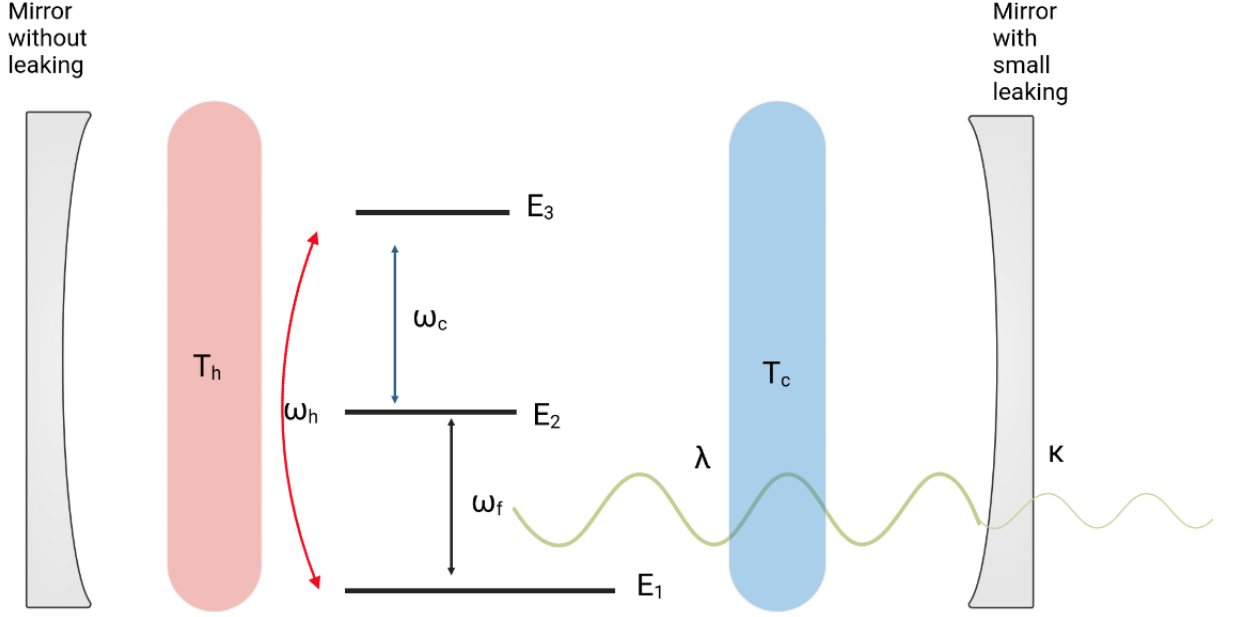


Figure 1: Schematic representation of a three-level maser heat engine continuously coupled to two reservoirs of temperatures  $T_h$ ; And  $T_c$ . And the three energy levels  $E_1, E_2, E_3$ . The system is interacting with a quantized single mode field.  $\lambda$  represents the strength of matter-field coupling.

A maser/laser consists of two elements. One of them is a gain medium and the other one is an optical resonator. A gain medium is always a material with an atomic transition between two atomic states. When an atom decays from an energetically higher state to an energetically lower state, a photon is created. In a three level system the three energy levels are  $E_1, E_2, E_3$  shown in Fig. 1. In a first part the system gets pumped from the lowest  $E_1$  level to the highest level  $E_3$ . The resonator should have a longer decay time, so that a population inversion can build up. This means that the system is in the energetically higher state. From this state they come almost exclusively through stimulated emission into the lower state  $E_1$ . The cavity is build of

two mirrors. One of the cavity have a small leaking, so that a small part of the photons can leave the cavity. This leaking is quantified by a constant  $\kappa$ . Our cavity is in resonance, therefore we set  $\omega_{cav} = \omega_f$ . Emission is a necessary condition for coherent light. Coherent light means all the photons have the same phase and same frequency [2].

Here we consider that higher level will be reached with a interaction of a hot bath. We denote the frequencies of  $\omega_h = (E_3 - E_1)/\hbar$ ,  $\omega_c = (E_2 - E_1)/\hbar$  and  $\omega_{cav} = (E_2 - E_1)/\hbar$ . In this three-level system each thermal photon from the bath trigger a lasing photon. The efficiency is given by the following formula:

$$\frac{J_{cav}}{J_h} = \eta_{maser} = \frac{\omega_{cav}}{\omega_h} < 1 - \frac{T_c}{T_h}. \quad (1)$$

## 2.2 Master-Equation

An arbitrary state of a cavity and a atom can be described by a total density operator  $\rho(t)$ . The complete description of the total system's state at a given time  $t$  is encoded in this density operator  $\rho$  [2]. The master equation is:

$$\dot{\rho}(t) = \frac{1}{i\hbar}[H, \rho] + \mathcal{L}_h\rho + \mathcal{L}_c\rho + \mathcal{L}_{cav}\rho. \quad (2)$$

To derive the  $\rho_{tot}$  we can solve a specific differential equation. This equation is called Lindblad-master-equation (2). The first part of eq (2) is the von Neuman equation, the analogue of the Schrödinger equation for density matrices. This part of the equation is unitary and therefore the process is reversible. The interaction with the various environmental heat baths is described by the non-unitary Liouvillian.  $\mathcal{L}_h$  describe the interaction with the hot bath,  $\mathcal{L}_c$  is the contribution from the interaction with the cold bath coupled with the atom.  $\mathcal{L}_{cav}$  describe the photons which are in the cavity. Those  $\mathcal{L}_{h,c,cav}$  are also called superoperators, which act on the density operator. A superoperator is a linear operator acting on a vector space of linear operator.  $\kappa$  describes the rate of photons which leave the cavity.  $H$  is the the Hamiltonian operator. The Hamiltonian describes the energy. The atomic field system is composed of two crucial parts; the atomic states, the cavity field, and the interaction between the two. The total Hamiltonian,

$$H = H_{free} + H_{int}, \quad (3)$$

consist of two parts; The part of the free Hamiltonian

$$H_{free} = \sum_{i=1}^3 \hbar\omega_i |i\rangle \langle i| + \hbar\omega_{cav} a^\dagger a, \quad (4)$$

and the interaction Hamiltonian or Jaynes-Cummings Hamiltonian:

$$H_{int} = \hbar g(\sigma_{12}a^\dagger + \sigma_{21}a). \quad (5)$$

The coupling constants  $g$  strong for the Hamiltonian and the  $\kappa$  for the Liou-villian part. The coupling constant is  $g$

The interaction with the various environmental heat baths is described by the Liouvillian:

$$\begin{aligned}\mathcal{L}_h\hat{\rho} &= \frac{\gamma_h}{2}(n(\omega_h, T_h) + 1) \cdot \mathcal{D}[\sigma_{13}]\rho + \frac{\gamma_h}{2}n(\omega_h, T_h) \cdot \mathcal{D}[\sigma_{31}]\rho \\ \mathcal{L}_c\hat{\rho} &= \frac{\gamma_c}{2}(n(\omega_c, T_c) + 1) \cdot \mathcal{D}[\sigma_{23}]\rho + \frac{\gamma_c}{2}n(\omega_c, T_c) \cdot \mathcal{D}[\sigma_{32}]\rho \\ \mathcal{L}_{cav}\hat{\rho} &= \kappa((\omega_{cav}, T_f) + 1) \cdot \mathcal{D}[a]\rho + \kappa n(\omega_{cav}, T_f) \cdot \mathcal{D}[a^\dagger]\rho.\end{aligned}\tag{6}$$

$\sigma_{12}$  is the transition operator and defined as  $|1\rangle\langle 2|$ . Similar for  $\sigma_{13} = |1\rangle\langle 3|$ ,  $\sigma_{23} = |2\rangle\langle 3|$ . The transition operator describe the transition between an atomic state  $a$  to  $b$ .  $\mathcal{D}$  is defined with following formula

$$\mathcal{D}[A]\rho = (2A\rho A^\dagger - A^\dagger A\rho - \rho A^\dagger A).\tag{7}$$

Where  $A$  represents one of the transition operators  $\sigma_{ab}$  or a ladder operator  $a$ . The Bose-Einstein occupation number. It is the mean number of excitations in the reservoir damping the oscillator. It describes the mean occupation number  $\langle n(E) \rangle$  of a quantum state of energy  $E$ , in thermodynamic equilibrium at absolute temperature  $T$  for identical bosons as occupying particles.  $n$  depends on the temperature and the frequency.  $n$  is defined as:  $n_i(\omega_i, T) = \frac{1}{\exp[\frac{\hbar\omega_i}{k_b T_i}] - 1}$ . The prefactor  $\gamma_c, \gamma_h$  describes the spontaneous decay rates and are in this calculation generally small. The Liouvillian has different constants. In this case the master equation is solved for the steady states. A steady state is a state or condition of a system or process, that the density matrix of the state does not change in time, or the changes are negligibly. Therefore all observables do not change in time either. It contains the whole description of the three-level system and the cavity.

## 3 Methods

### 3.1 Implementation of the three-level-system in qutip

Qutip can be used to solve master equations. To use the qutip functions, it is important to define the constants first. In our case, only the transition between  $|1\rangle$  and  $|2\rangle$  interact with the light. Defined as constants are the three different Bose-Einstein occupation  $n_h, n_c$  and  $n_f$ . The transition-operators  $\sigma_{ab}$  are made by qutip implementation of the tensor product of  $|a\rangle\langle b|$  and the identity matrices of size of maximum photon number. In the same way, I implemented the other transition operators and  $|1\rangle$  and  $|2\rangle$  are basis states. For our purpose, it will always suffice to truncate the photon's Hilbertspace of  $n = 30$ . So we get 90 x 90 matrices. The projectors are

implemented similarly, with the matrix  $|a\rangle\langle a|$ . With those it is easy to construct the Hamiltonians,  $H_{free}$  and  $H_{int}$ , as in Eq. (4), Eq. (5). To calculate the density matrices for steady states we can also use a qutip function. This function needs the total Hamiltonian and a list of the non-unitary operators as arguments. As output of the function steady-state we get the density-matrices for steady-states. [3]

## 4 Lasing transition

### 4.1 Wigner function and phase-averaged coherent states

The output of a laser is coherent light. The quantum description of coherent light is a coherent state. The photon number distribution of coherent light is a Poisson distribution. In our case the output is a phase-averaged coherent state (PHAV). That's a coherent state which has an averaged phase  $\phi$  around  $2\pi$ . Randomizing the phase of a coherent state doesn't change the photon-number distribution.

A Wigner function is a representation of a general quantum state of light [1]. The function describes the probability density in phase space.

$$w(x, p) = \frac{1}{2\pi\hbar} \int_{-\infty}^{\infty} d\xi e^{\frac{-ip\xi}{\hbar}} \langle x + \frac{1}{2}\xi | \rho | x - \frac{1}{2}\xi \rangle. \quad (8)$$

The Wigner function from a coherent state is a Gaussian. The Wigner function of a coherent and a phase-average-state is non-Gaussian, because  $p_{nn}$  of Eq. (10) is a Poisson distribution. So we get a new term of  $\exp(i\pi\phi)$  in it. The standard coherent state  $|\alpha\rangle$  can be represented by following formula:

$$|\alpha\rangle = e^{\frac{-|\alpha|^2}{2}} \sum_{n=0}^{\infty} \frac{|\alpha|^n e^{in\phi}}{\sqrt{n!}} |n\rangle. \quad (9)$$

Get the PHAV state will be obtained by integrating over the phase  $\phi$ .

$$\rho_{PHAV} = \int_0^{2\pi} \frac{d\phi}{2\pi} |\alpha(\phi)\rangle \langle \alpha(\phi)| = \sum_{n=0}^{\infty} p_{nn} |n\rangle \langle n|, \quad (10)$$

thus is equal to

$$\rho_{PHAV} = \sum_{n=0}^{\infty} \exp(-|\alpha|^2) \frac{|\alpha|^{2n}}{n!} |n\rangle \langle n|. \quad (11)$$



Eq. (11) is implemented in python to visualize a photon number distribution and Wigner plot Eq (8), shown in Fig 4.1. A Fock plot shows the occupation probability  $p_{nn}$ .

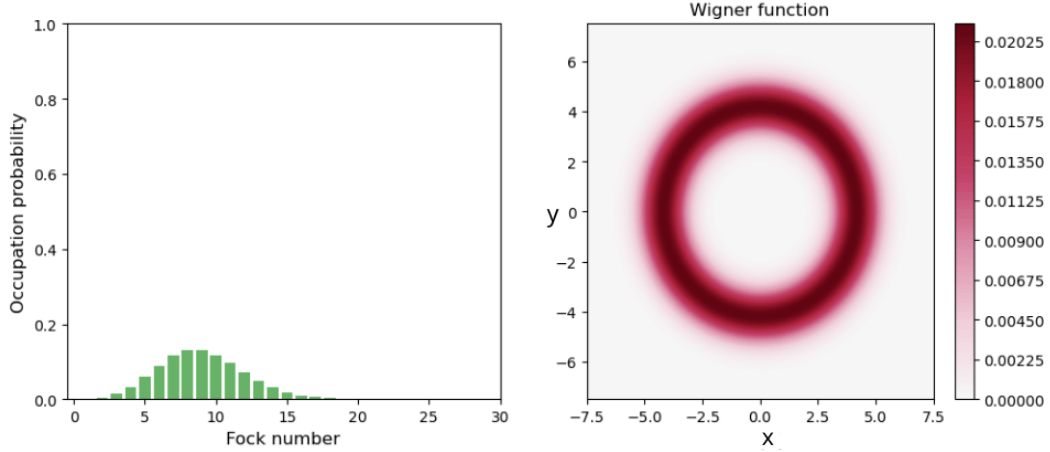


Figure 2: The Wigner-Fock plot of the density matrix of  $\rho_{PHAV}$  with the parameter  $\alpha = 3.5$ .

For the Wigner function (8) we finally get the following equation

$$w(x, p) = 2 \exp[-2(|\alpha|^2 + |x + ip|^2)] I_0(4|\alpha||x + ip|). \quad (12)$$

$I_0$  is the first Bessel function. This function is plotted in Fig. 2. The first result are plots from the photon number distribution and the Wigner function. For all calculations, I set the parameters  $\hbar$  and  $kb$  equal to one.  $\gamma_h, \gamma_c$  are set to 1. And  $\kappa = 0.028\gamma_h$  I tested those with different set of parameters, shown in Fig. 3 and Fig. 5.

Those rings which are shown in Fig. 3 and Fig. 5, are similar to the plot of Fig. 2. If we have a small  $\kappa$  means less photons will not leave and stay in the cavity. we see that in the plot of the photon number distribution. In the first plot I set a high leaking-parameter  $\kappa = \frac{1}{\gamma_h}$ . Shown in Fig. 3. This means that many photons leave the cavity, and only a few remain in the cavity. We see, that the occupation-number the photon number distribution is most zero and the probability for one photon is just 0.1.

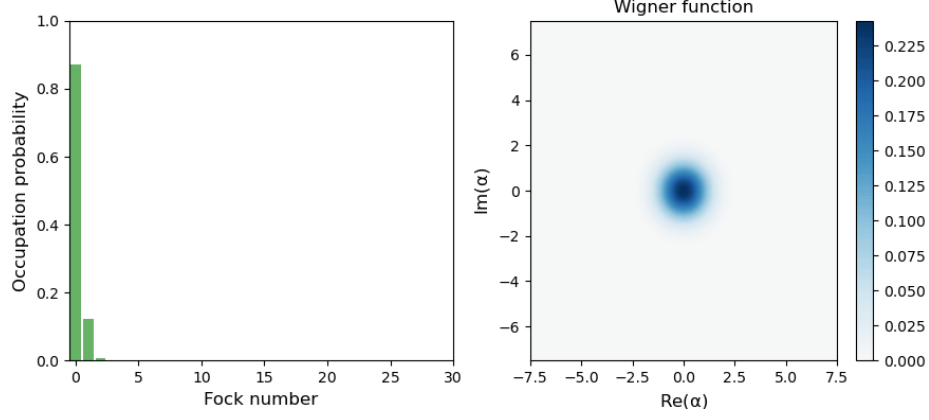


Figure 3: The parameters for the first plot are  $n_h = 2.6, n_c = 0.001, n_f = 0.02, \kappa = 1\gamma_h$ . With the factor of  $\kappa = 1\gamma_h$  the leaking is too high for a lasing state.

In the second plot I took the same parameters again, but with a lower  $\kappa$ . We get more photons in the cavity. We see the distribution in the photon number distribution plot and a PHAV state in the Wigner function.

## 4.2 Double threshold behaviour and population inversion

The population inversion is seen by calculating the probability for the occupation number ( $Tr[|i\rangle\langle i|\rho]$ ) and  $i$  stands for the different occupation of the state. Fig. 4a. With high  $n_h$  the probability for the system to stay in a the state  $|2\rangle$  increases as well. Because the transition between the  $E_2$  and  $E_1$  happened by photon emission and this emission rate is slower as the decay rate from  $E_3$  to  $E_2$ . A interesting phenomena of the lasing output is the double threshold behaviour Lasing starts once a threshold for emission is attained, however, increasing the heat flow too much will end up producing thermal light instead of lasing. This phenomena is called a double threshold behaviour.[2] To investigate this double threshold behaviour, we study the steady states of a three-level system. This double threshold behaviour can can be explained by the Zeno effect. The Zeno effect describes that the transition from one state to the other can be stopped by rapid successive measurements. The system behaves similarly when sufficient stimulation is applied quickly. With the plot  $Tr[n\rho] = \langle n \rangle$  against different  $n_h$  Fig. 4b we see this double threshold behaviour because, when the hot bath temperature  $n_h$  is too low ( $n_h \approx n_c$ ) we have also a low photon number. With increasing  $n_h$ , population inversion happens, the photon number increase and the output looks like a PHAV state, see Fig. 2. With too high  $n_h$  the expected photon number decrease again and this system shows a double threshold behaviour, the excitation is too weak, and we say that the system is below the lasing threshold. This is another critical point, after which the output light becomes thermal radiation.

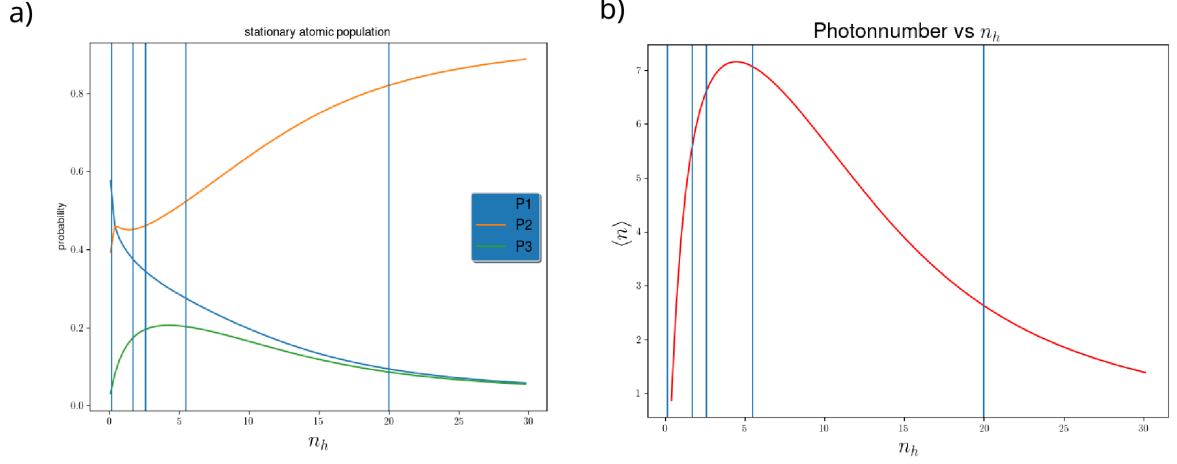


Figure 4: In Fig. 4a the probability for an atom to stay in a state  $|0\rangle, |2\rangle$  or  $|3\rangle$  vs  $n_h$  with the parameters. With a increasing  $n_h$   $P2$  increase as well. We call it population inversion. The parameters for the first plot are  $n_c = 0.02, n_f = 0.02, \kappa = 0.01\gamma_h$ . The blue lines mark the the values for  $n_h$  for which the Wigner functions are plotted. In Fig. 4b we see, the the expectation value of the photon number versus different  $n_h$

In a first step, the reduce density matrices  $\rho_{free}$  will be used to make Wigner and Fock plots.  $\rho_{free} = Tr_{H_{free}}[\rho]$ . It is possible to make the partial trace of  $\rho$  with qutip, to trace out the reduced density matrices  $\rho_{free}$ .

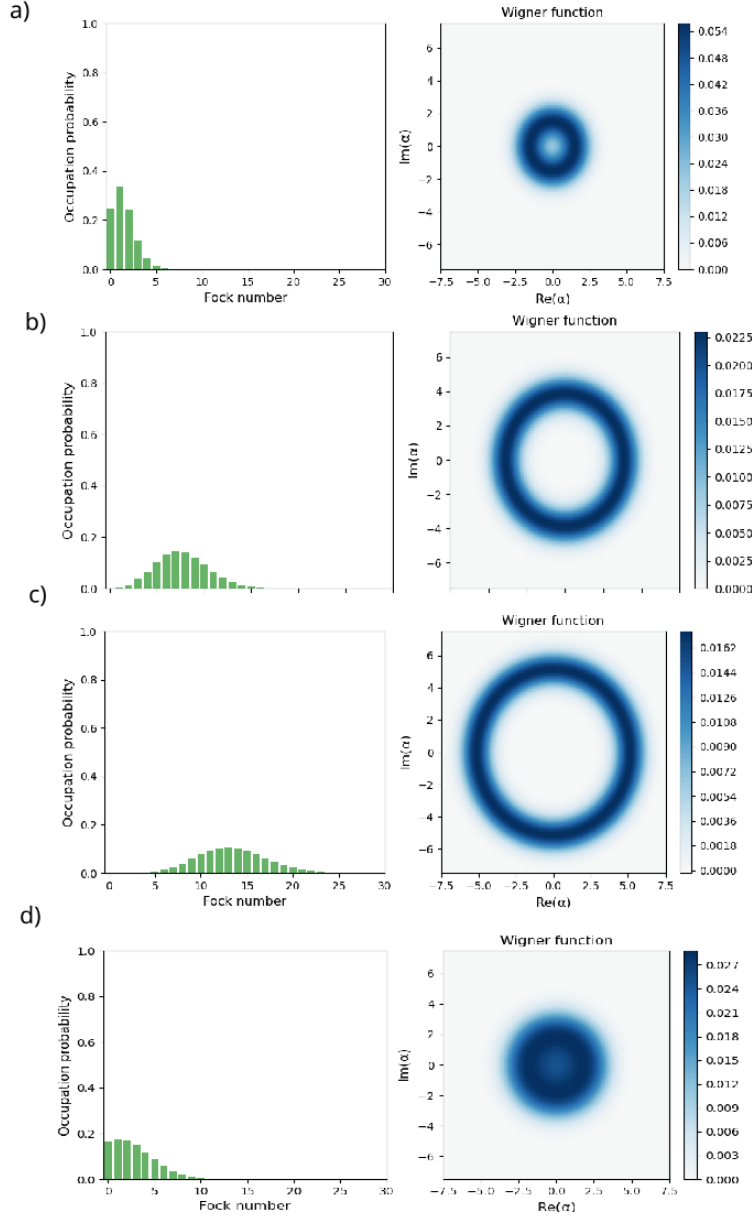


Figure 5: For all of the four the parameters are  $n_c = 0.001n_f = 0.02, \kappa = 0.1\gamma_h$ . Cavity with a small leaking. **a)** The parameters for  $n_h$  are  $n_h = 0.2$ . **b)**  $n_h = 2.6$  **c)**  $n_h = 5.5$  **d)**  $n_h = 20$ .

We see in Fig 5a that start to get a PHAV If we increase  $20 > n_h \gg 0.2$ , then the cavity photon number increases again when increasing  $n_h$  at the very high temperature regime, as shown in Fig. 5b, Fig 5c. Because, in this

regime, the system has already a population inversion thus the increase of the hot bath temperature  $T_h$  can no longer bring in a significant increase to the photons gain. The hot bath no longer has any weakening effect to the lasing, thus more lasing photons can be produced in the cavity, and the lasing power can be increased. But, still, the cavity photon number is limited due to the single atom feature. If we further increase  $n_h > 10$ , we see the double threshold behavior. In Fig. 5d we get by  $n_h = 20$  a thermal state.

## 5 Thermodynamics

### 5.1 Heat currents

When we work with density matrices, it is common to work with expectation values with  $\langle A \rangle = \text{Tr}[A\rho]$ .  $A$  is an operator and describe a measurement. With this, we can calculate the expectation value from an Operator. To calculate the expected heat flow we can take the partial trace from  $\text{Tr}[H_{free}, \mathcal{L}[\rho]]$ .

$$\langle J_{tot} \rangle = \text{Tr}[H_{free} \cdot \mathcal{L}_h[\rho]] + \text{Tr}[H_{free} \cdot \mathcal{L}_c[\rho]] + \text{Tr}[H_{free} \cdot \mathcal{L}_{cav}[\rho]]. \quad (13)$$

A part of my work is to calculate the occupation number analytically. The calculation is made in two steps. For the warm and the cold bath, we have a transition-operators in the trace. The trick of this calculation is, to get the form  $\text{Tr}[\sigma_{ab}\rho\sigma_{ab}^\dagger]$ . The equation gave the following result:

$$\langle J_h \rangle = \text{Tr}[H_{free} \cdot \mathcal{L}_h[\rho]] = \hbar\omega_h\gamma_h(2n_h + 1)(P1 - P3), \quad (14)$$

The same calculation can be done for the interaction with the cold bath.

$$\langle J_c \rangle = \text{Tr}[H_{free} \cdot \mathcal{L}_c[\rho]] = \hbar\omega_c\gamma_c(2n_c + 1)(P2 - P3), \quad (15)$$

For the calculation the  $\text{Tr}[H_{free} \cdot \mathcal{L}_{cav}[\rho]]$ , I get the following result

$$\langle J_{cav} \rangle = \text{Tr}[H_{free} \cdot \mathcal{L}_{cav}[\rho]] = 2\hbar\omega_{cav}\kappa(n_{cav} - \langle a^\dagger a \rangle). \quad (16)$$

With the density matrices it is possible to calculate the heat flux by taking  $\text{Tr}[H\mathcal{L}\rho]$ . and plot this for different  $g$  so the goal of this work is to find a  $n_h$  which yield a PHAV state, as in [1] In the second step of the calculation we look for  $\langle J_{tot} \rangle$  on different coupling constants  $g$ . In other words, in the plot below, the Trace from the density matrices times the Liouvillian against the coupling constant is visualized. The master equation depends on three different Liouvillian terms. I calculated the expected heat flow for every different interaction. The cold interaction, the warm and the interaction with the cavity. Fig. 6 shows for the parameters  $n_h = n_c = 2.6n_f = 0.02$ ,  $\kappa = 0.01$  is shown below.

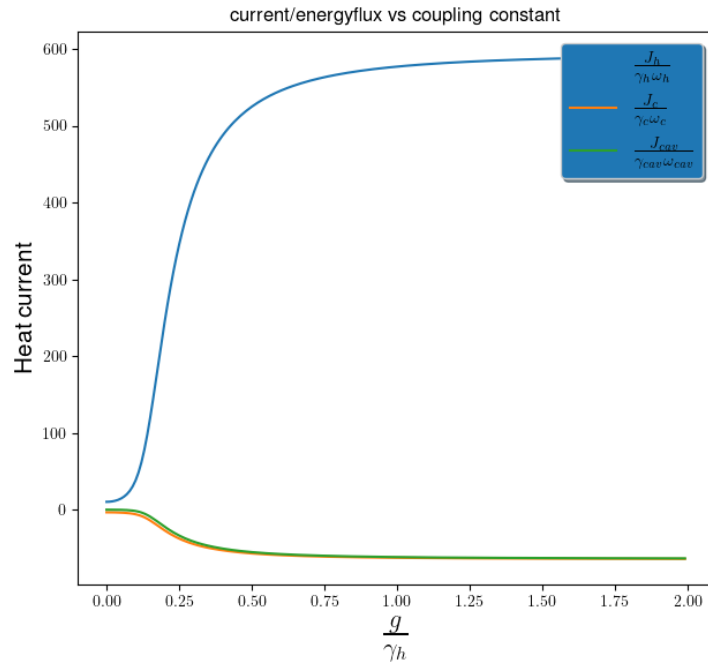


Figure 6: Energy flux vs  $g$  with the parameters The parameters for the first plot are  $n_h = 2.6, n_c = n_f = 0.02, \kappa = 0.01$

## 5.2 Entropy production

Another relevant concept is the entropy. It is also a physical property. The entropy production is given by the formula  $\dot{\sigma} = \frac{J(n_h)}{T(n_c)} + \frac{J(n_c)}{T(n_h)} + \frac{J(n_{cav})}{T(n_{cav})}$ . As already seen in Fig. 4b we have a optimum parameter  $n_h$ . in Fig. 4a we see the probability for  $P1, P2, P3$  is in the region of  $n_h = 5$  well distributed. We see also that this corresponds with the average of the photon number. The higher the entropy, the more the state of the three-level system changes and the more photons are emitted. We see that the entropy production correlate with the average of photon number in Fig 4b.

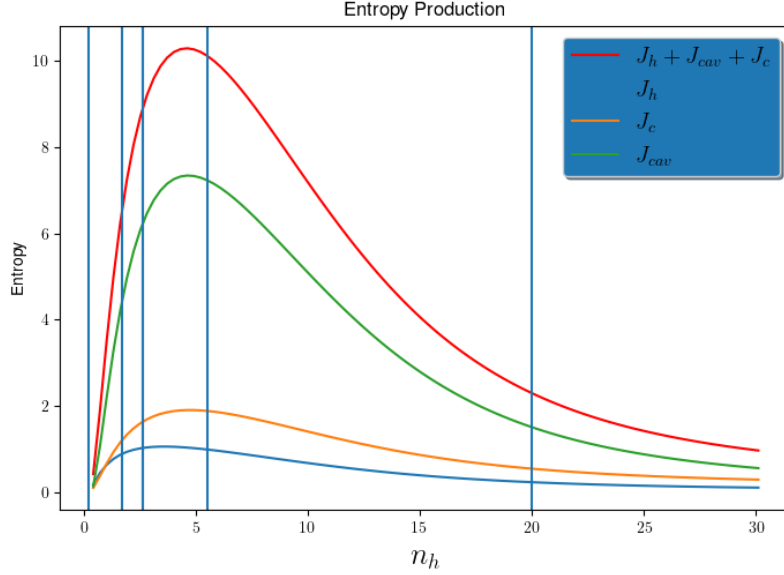


Figure 7: The entropy production for different  $n_h$ . The parameters for the first plot are  $n_c = 0.001n_f = 0.02, \kappa = 1$ . As in paper [2] is used the values for the frequencies  $\omega_f = 30\frac{1}{t}, \omega_h = 150\frac{1}{t}, \omega_c = 120\frac{1}{t}$ .



## 6 Conclusion and outlook

In those numerical calculations are found PHAV states in a cavity, driven by the coupling of two different thermal bath. We found the double threshold behaviour from the system, by calculating different energy flux for different  $n_h$ . As in the paper [2]. With the condition that  $n_c, n_{cav}$  is almost zero, the leaking  $\kappa$  is small too, and the hot bath received a value between 1 and 5.5. When we compare the Wigner functions of the numerical calculated states from a our three-level system Fig 4b,4c with the Wigner plot of a PHAV state Fig. 2, we see, that they are pretty similar. As conclusion; it's possible to get a phase average coherent state. In Fig. 6 we see the average of the current, calculated with the formula Eq. (13) for different coupling constants  $g$ . The conclusion from Fig. 6 is, that the current increase at most between the  $0 < g < 0.25$ . In Fig. 4a we see the probability in which state the system is. If we increase the temperature from the hot bath, we see that the occupation probability of  $P2$  increase as well. A population inversion is visible. Fig. 4 helps to get some conclusion about the system starts lasing and when it stops. With a too small temperature, It has not enough energy in the system and the photon number is low Fig 4a. If  $n_h$  increase more, a maximum lasing output is reached Fig 4b,4c. If the temperature increasing further, the system is in the highest level, therefore the Rabi oscillation between  $E_0$  and  $E_2$  does not exist anymore and we get a thermal state Fig 4d. At higher heat of the warm bath, dephasing of the system occurs. Thus, it interacts more with the environment. This has the same effect as if the system is measured often. The Zeno effect then make that the system no longer oscillates between two different states. The consistent numerical and theoretical results we have obtained in the characterization of both PHAV states. A motivation to get those PHAV states is; with two PHAV states reinforce the possibility of using them for applications to communication protocols [1]. In further calculation we will look at the thermodynamic uncertainty relation (TUR) and a second laser as input.

## References

- [1] Alessia Allevi et al. "Characterization of phase-averaged coherent states". In: *Journal of the Optical Society of America B* 30.10 (2013), p. 2621. ISSN: 0740-3224. DOI: 10.1364/josab.30.002621. arXiv: 1302.2011.
- [2] Sheng Wen Li et al. "Quantum statistics of a single-atom Scovil-Schulz-DuBois heat engine". In: *Physical Review A* 96.6 (2017), pp. 1–10. ISSN: 24699934. DOI: 10.1103/PhysRevA.96.063806. arXiv: 1710.00902.

- URL: <http://arxiv.org/abs/1710.00902><http://dx.doi.org/10.1103/PhysRevA.96.063806>.
- [3] P. D. Nation and J. R. Johansson. “QuTiP: Quantum Toolbox in Python 4.7.0”. In: *QuTip* (2022), p. 241. URL: <http://qutip.org/documentation.html>.
  - [4] Marco Scigliuzzo et al. “Primary Thermometry of Propagating Microwaves in the Quantum Regime”. In: *Physical Review X* 10.4 (2020), p. 41054. ISSN: 21603308. DOI: 10.1103/PhysRevX.10.041054. arXiv: 2003.13522. URL: <https://doi.org/10.1103/PhysRevX.10.041054>.
  - [5] H. E.D. Scovil and E. O. Schulz-Dubois. “Three-level masers as heat engines”. In: *Physical Review Letters* 2.6 (1959), pp. 262–263. ISSN: 00319007. DOI: 10.1103/PhysRevLett.2.262. URL: <https://link.aps.org/doi/10.1103/PhysRevLett.2.262>.

## 7 Appendix

The hole Master equation without any substitution:

$$\begin{aligned}
\mathcal{L}\hat{\rho} = & \frac{\gamma_h}{2} \left[ \frac{1}{\exp[\frac{\hbar\omega_h}{k_b T_h}] - 1} + 1 \right] \cdot \left( 2\sigma_{13} \cdot \rho \cdot \sigma_{13}^\dagger - \sigma_{13}^\dagger \sigma_{13} \rho - \rho \sigma_{13}^\dagger \sigma_{13} \right) \\
& + \frac{\gamma_h}{2} \left[ \frac{1}{\exp[\frac{\hbar\omega_h}{k_b T_H}] - 1} \right] \cdot \left( 2\sigma_{31} \cdot \rho \cdot \sigma_{31}^\dagger - \sigma_{31}^\dagger \sigma_{31} \rho - \rho \sigma_{31}^\dagger \sigma_{31} \right) \\
& + \frac{\gamma_c}{2} \left[ \frac{1}{\exp[\frac{\hbar\omega_c}{k_b T_c}] - 1} + 1 \right] \cdot \left( 2\sigma_{23} \cdot \rho \cdot \sigma_{23}^\dagger - \sigma_{23}^\dagger \sigma_{23} \rho - \rho \sigma_{23}^\dagger \sigma_{23} \right) \\
& + \frac{\gamma_c}{2} \left[ \frac{1}{\exp[\frac{\hbar\omega_c}{k_b T_c}] - 1} \right] \cdot \left( 2\sigma_{32} \cdot \rho \cdot \sigma_{32}^\dagger - \sigma_{32}^\dagger \sigma_{32} \rho - \rho \sigma_{32}^\dagger \sigma_{32} \right) \\
& + \kappa \left[ \frac{1}{\exp[\frac{\hbar\omega_f}{k_b T_f}] - 1} + 1 \right] \cdot \left( 2a\rho a^\dagger - a^\dagger a \rho - \rho a^\dagger a \right) \\
& + \kappa \left[ \frac{1}{\exp[\frac{\hbar\omega_f}{k_b T_f}] - 1} \right] \cdot \left( 2a^\dagger \rho a - a a^\dagger \rho - \rho a a^\dagger \right)
\end{aligned} \tag{17}$$

### 7.1 Software

For the implementation of the three-level-system in a cavity, I used qutip. Qutip is a python library, which allows to solving master equation fast. Further calculations and methods were easily applied in python.

$$\begin{aligned}
& \text{Tr} [H_{\text{free}} \cdot \mathcal{L}_h g] \\
&= \text{Tr} \left[ \sum_{i=0}^3 \hbar \omega_i |i\rangle \langle i| + \hbar \omega_2 a^\dagger a \right] \left( \frac{\gamma_h}{2} [n(\omega_h, T_h) + 1] \cdot (2 \bar{\sigma}_{13} g \bar{\sigma}_{13}^\dagger - \bar{\sigma}_{13}^\dagger \bar{\sigma}_{13} g - g \bar{\sigma}_{13}^\dagger \bar{\sigma}_{13}) + \right. \\
&\quad \left. + \frac{\gamma_h}{2} [\bar{n}(\omega_h, T_h)] (2 \bar{\sigma}_{31} g \bar{\sigma}_{31}^\dagger - \bar{\sigma}_{31}^\dagger \bar{\sigma}_{31} g - g \bar{\sigma}_{31}^\dagger \bar{\sigma}_{31}) \right) \\
&= \text{Tr} \left[ \hbar \omega_h \frac{\gamma_h}{2} (n(\omega_h, T_h) + 1) (|3\rangle \langle 3| 2 \bar{\sigma}_{13} g \bar{\sigma}_{13}^\dagger - |3\rangle \langle 3| \bar{\sigma}_{13}^\dagger \bar{\sigma}_{13} g - |3\rangle \langle 3| g \bar{\sigma}_{13}^\dagger \bar{\sigma}_{13}) \right. \\
&\quad + \text{Tr} \left[ \hbar \omega_h \frac{\gamma_h}{2} n(\omega_h, T_h) (|3\rangle \langle 3| 2 \bar{\sigma}_{31} g \bar{\sigma}_{31}^\dagger - |3\rangle \langle 3| \bar{\sigma}_{31}^\dagger \bar{\sigma}_{31} g - |3\rangle \langle 3| g \bar{\sigma}_{31}^\dagger \bar{\sigma}_{31}) \right. \\
&\quad + \text{Tr} \left[ \hbar \omega_c \frac{\gamma_h}{2} (n(\omega_h, T_h) + 1) (|1\rangle \langle 1| 2 \bar{\sigma}_{13} g \bar{\sigma}_{13}^\dagger - |1\rangle \langle 1| \bar{\sigma}_{13}^\dagger \bar{\sigma}_{13} g - |1\rangle \langle 1| g \bar{\sigma}_{13}^\dagger \bar{\sigma}_{13}) \right. \\
&\quad + \text{Tr} \left[ \hbar \omega_c \frac{\gamma_h}{2} n(\omega_h, T_h) (|1\rangle \langle 1| 2 \bar{\sigma}_{31} g \bar{\sigma}_{31}^\dagger - |1\rangle \langle 1| \bar{\sigma}_{31}^\dagger \bar{\sigma}_{31} g - |1\rangle \langle 1| g \bar{\sigma}_{31}^\dagger \bar{\sigma}_{31}) \right. \\
&\quad \left. + \text{Tr} [\hbar \omega_2 |2\rangle \langle 2| \cdot \mathcal{L}_h g] \right] = 0 \\
&\quad + \text{Tr} [\hbar \omega_h a \cdot \mathcal{L}_h g] = 0 \quad // \text{Kommutiert} \\
&= \text{Tr} \left[ \hbar \omega_h \frac{\gamma_h}{2} (n(\omega_h, T_h) + 1) (2 \cdot |3\rangle \langle 3| \bar{\sigma}_{13} g \bar{\sigma}_{13}^\dagger - |3\rangle \langle 3| \bar{\sigma}_{13}^\dagger \bar{\sigma}_{13} g - |3\rangle \langle 3| g \bar{\sigma}_{13}^\dagger \bar{\sigma}_{13}) \right. \\
&\quad + \text{Tr} \left[ \hbar \omega_h \frac{\gamma_h}{2} n(\omega_h, T_h) \cdot (2 |3\rangle \langle 3| 3\rangle \langle 1| g \bar{\sigma}_{13}^\dagger) = 4 (2 \cdot \bar{\sigma}_{31} g \bar{\sigma}_{13}^\dagger) = 4 P_1 \right. \\
&\quad + \text{Tr} \left[ \hbar \omega_c \frac{\gamma_h}{2} n(\omega_h, T_h) \cdot |1\rangle \langle 1| (2 \cdot \bar{\sigma}_{13} g \bar{\sigma}_{13}^\dagger) = 2 |1\rangle \langle 1| 1\rangle \langle 3| g |3\rangle \langle 1| = 2 P_3 \right. \\
&\quad \left. + \text{Tr} \left[ \hbar \omega_c \frac{\gamma_h}{2} n(\omega_h, T_h) \cdot |1\rangle \langle 1| 2 \bar{\sigma}_{31} g \bar{\sigma}_{31}^\dagger - |1\rangle \langle 1| g \bar{\sigma}_{31}^\dagger \bar{\sigma}_{31} g = -2 P_1 \right. \right. \\
&\quad \left. \left. - |3\rangle \langle 3| g \bar{\sigma}_{13}^\dagger \bar{\sigma}_{13} = g |3\rangle \langle 1| 1\rangle \langle 3| = P_3 \right. \right. \\
&\quad \left. \left. \begin{aligned} &= -\hbar \omega_h \gamma_h \cdot n(\omega_h, T_h) + 1 \cdot P_3 \\ &+ \hbar \omega_h \gamma_h \cdot n(\omega_h, T_h) \cdot P_3 \end{aligned} \right\} = -\hbar \omega_h \gamma_h P_3 \right. \\
&\quad \left. \left. \begin{aligned} &+ \hbar \omega_c \gamma_h \cdot (n(\omega_h, T_h) + 1) \cdot P_1 \\ &- \hbar \omega_c \gamma_h \cdot n(\omega_h, T_h) \cdot P_2 \end{aligned} \right\} = +\hbar \omega_c \gamma_h P_1 \right. \\
&= \hbar \gamma_h \cdot (\omega_c P_1 - \omega_h P_3)
\end{aligned}$$

Figure 8: Berechnung-Tr[HL]

$$\begin{aligned}
& \text{Tr} [H_{\text{tree}} \cdot \mathcal{L}_{\text{cav}} g] \\
&= \left( \sum_{i \leftarrow d} \hbar \omega_i |i\rangle \langle i| + \hbar \omega a^\dagger a \right) \cdot [k(\bar{n}+1) \cdot (2 a g a^\dagger - a^\dagger a g - g a^\dagger a)] \\
&+ \left( \sum_{i \leftarrow d} \hbar \omega_i |i\rangle \langle i| + \hbar \omega a^\dagger a \right) \cdot [k \bar{n} \cdot (2 a^\dagger g a - a a^\dagger g - g a a^\dagger)] \\
&= \text{Tr} [\hbar \omega k(\bar{n}+1) [2 a^\dagger a a g a^\dagger - a^\dagger a a^\dagger a g - a^\dagger a g a^\dagger a] \\
&+ \hbar \omega k \bar{n} [2 a^\dagger a a^\dagger g a - a^\dagger a a^\dagger a g - a^\dagger a g a a^\dagger] \\
&= \hbar \omega k(\bar{n}+1) [2 \text{Tr} a^\dagger a^\dagger a a g] \ominus 2 \text{Tr} [a^\dagger a a^\dagger a g] \quad \begin{matrix} \nearrow 2 \text{Tr} [a^\dagger a g] - \text{Tr} [a^\dagger a a a] \\ 0_a \quad a a^\dagger - a^\dagger a = 1 \end{matrix} \\
&+ \hbar \omega k \bar{n} \cdot [2 \text{Tr} [a a^\dagger a a^\dagger g] - \text{Tr} [a^\dagger a a^\dagger a g] - \text{Tr} [a a^\dagger a^\dagger g] \\
&= \hbar \omega k(\bar{n}+1) \cdot \text{Tr} [a^\dagger a g] \\
&+ \hbar \omega k \bar{n} \cdot \text{Tr} [a a^\dagger (a a^\dagger - a^\dagger a) g] + \text{Tr} [a a^\dagger a a^\dagger g] - \text{Tr} [a^\dagger a a a^\dagger g] \\
&= \hbar \omega k(\bar{n}+1) 2 \text{Tr} [a^\dagger a g] + \\
&+ \hbar \omega k \bar{n} [2 \text{Tr} [a a^\dagger g] + \text{Tr} [(a a^\dagger - a^\dagger a) a a^\dagger g] \\
&= \hbar \omega k(\bar{n}+1) 2 \text{Tr} [a^\dagger a g] + \hbar \omega k \bar{n} 2 \text{Tr} [a a^\dagger g] \\
&= 2 \hbar \omega k (\bar{n} - \langle a^\dagger a \rangle)
\end{aligned}$$

Figure 9: Berechnung- $\text{Tr}[\text{HL}]$ .